34th Annual International Conference of the IEEE EMBS
San Diego, California USA, 28 August - 1 September, 2012

Automated Boundary Extraction of the Spinal Canal in MRI Based on Dynamic Programming*

Jaehan Koh[1], Vipin Chaudhary[2] and Gurmeet Dhillon, MD[3]

Abstract— **The spinal cord is the only communication link between the brain and the body. The abnormalities in it can lead to severe pain and sometimes to paralysis. Due to the growing gap between the number of available radiologists and the number of required radiologists, the need for computer-aided diagnosis and characterization is increasing. To ease this gap, we have developed a computer-aided diagnosis and characterization framework in lumbar spine that includes the spinal cord, vertebrae, and intervertebral discs. In this paper, we propose two spinal cord boundary extraction methods that fit into our framework based on dynamic programming in lumbar spine MRI. Our method incorporates the intensity of the image and the gradient of the image into a dynamic programming scheme and works in a fully-automatic fashion. The boundaries generated by our method is compared against reference boundaries in terms of Fréchet distance which is known to be a metric for shape analysis. The experimental results from 65 clinical data show that our method finds the spinal canal boundary correctly achieving a mean Fréchet distance of 13.5 pixels. For almost all data, the extracted boundary falls within the spinal cord. So, it can be used as a landmark when marking background regions and finding regions of interest.**

I. INTRODUCTION

There is a growing concern about the lack of diagnostic radiologists due to the linear growth of the number of available radiologists compared to the exponential growth of the number of required radiologists [1]. Therefore, there is an increasing need for the effective computer-aided management of pathology in lumbar spine using multi-protocol MR images.

Magnetic resonance imaging (MRI) is known to be the most effective primary diagnostic tool in the clinical evaluation of the lumbar spine since it provides more anatomic sources of pain including nerves, muscles, and ligaments than X-ray or computed tomography (CT). Interestingly, some clinical studies show that computer-aided diagnosis (CAD) enhances the number of cancer detection by about 10% which is similar to double reading by two radiologists [2]. To this end, we have developed a CAD framework, LumbarDiagnostics, for computer-aided characterization and diagnosis of lumbar spine pathology using multi-protocol MRI in a reliable and rapid manner.

The spinal cord is a crucial communication path between the brain and the body. This cylindrical structure of nervous tissues is clinically important as several diseases can develop in this region resulting in pain and sometimes in paralysis. In a sagittal view, the spinal cord reaches around the level $L2$ and the dural sac wrapping around the spinal cord terminates around the level $S2$ as in Fig. 1 (a). In our framework, the spinal canal including the spinal cord and the dural sac is used as a landmark region that aids to locate a region of interest (ROI) and to localize neighboring vertebrae and intervertebral discs because of its high brightness. Thus, the spinal canal segmentation in an accurate, fast and automated fashion is a crucial preprocessing step for the localization of neighboring vertebrae and intervertebral discs and feature generation for pathology diagnosis in lumbar spine.

Since a T1-weighted sagittal image and a corresponding T2-weighted image are co-registered, the intensity difference between them is known to give a clear snapshot of the boundary of the spinal canal as in Fig. 1(b) [12]. Thus, we use this difference image for tracing spinal canal boundaries in two different ways: one based on intensity values of the image, and the other based on the gradient of the image. As in Fig. 1(c) and Fig. 1(d), the dynamic programming help trace the boundary of the spinal canal which is part of regions of interest. This boundary is used in background region removal and localization of lumbar pathology.

A. Related Work

There have been many efforts in boundary tracing and extraction in diverse modalities. Geiger et al. [3] provided a segmentation method based on dynamic programming and a multi-scale approach. They also demonstrated the algorithms on natural objects in a set of applications, including interactive segmentation and automatic tracking of the regions of interest in medical images. Liang et al. [4] presented an automated boundary tracing method aiming at reducing inter-observer variability by applying a multi-scale dynamic programming algorithm. They claimed that this automated procedure can replace the manual procedure with improved performance. Kirbas and Quek [5] provided a survey of vessel extraction techniques and algorithms based on several modalities. They have comprehensively divided vessel segmentation algorithms into six main categories.

Regarding the spinal cord area, most of the work focused on the segmentation problem of the spinal cord and the spinal

*This work is supported in part by grants from NSF and NYSTAR.

[1]J. Koh is with the Department of Computer Science and Engineering, University at Buffalo, SUNY, Buffalo, NY 14228, USA jkoh@buffalo.edu

[2]V. Chaudhary is with Faculty of the Department of Computer Science and Engineering, University at Buffalo, SUNY, Buffalo, NY 14228, USA vipin@buffalo.edu

[3]G. Dhillon is with Proscan Imaging of Buffalo, Williamsville, NY 14221, USA gdhillon@proscan.com

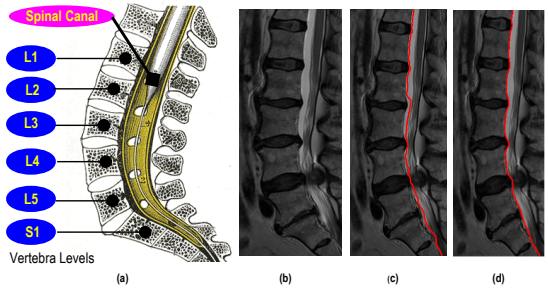

Fig. 1. (a) Lumbar spine anatomy [14], (b) a T2-weighted sagittal image, (c) an output boundary overlaid on an input image by the intensity-based method, and (d) an output boundary overlaid on an input image by the gradient-based method.

canal in MRI than boundary tracing. Some of the recent attempts are as follows. Schmit and Cole [6] proposed a semi-automatic segmentation method of the spinal cord in MRI. Given initial seed points, the three-dimensional region growing is followed. The careful selection of initial points determines the performance of this method. Uitert et al. [7] proposed a semi-automatic process for the the spinal cord segmentation in MRI. This method has a limitation that seed points along the center of the spinal cord need to be provided by a human being. McIntosh and Hamarneh [8] presented a semi-automatic framework for segmentation and analysis of the spinal cord in MRI using multi layers. The framework was validated quantitatively but it took a relatively long execution time (i.e., about 10 minutes) and required seed points. Recently, Horsefield et al. [9] reported a semi-automatic segmentation of the spinal cord from MRI. The method was validated through intra-observer reproducibilities, but it required approximate centerline of the spinal cord by a user. The above methods are not fully automatic or the segmentation results are not validated quantitatively. However, our boundary extraction methods work in a fully automatic way and the output of the method is quantitatively evaluated by a performance metric.

This paper is organized as follows. In Section 2, our CAD framework and two boundary extraction methods are presented. Then in Section 3, experimental results and discussion will be given. Finally, Section 4 concludes the paper.

II. METHODS

A. LumbarDiagnositcs *Framework*

The proposed methods work within the LumbarDiagnostics for computer-aided characterization and diagnosis of lumbar spine pathology using multi-protocol MRI in a reliable and rapid manner.

The framework consists of meta data analysis, inter- and intra-slice analysis, preprocessing, regions of interest determination, and reference generation. The detailed tasks within each step are as follows.

•**Meta Data Analysis.** Available protocol information is extracted from the Digital Imaging and Communications in Medicine (DICOM) header of each MR slice image.

•**Inter- and Intra-slice Analysis.** This step concerns about finding the best slice that gives the clear snapshot of the lumbar structure for characterization and diagnosis. By the best slice we mean that the best image for diagnosis. In the sagittal plane, the mid-sagittal image usually clearly depicts the boundaries of vertebrae, intervertebral discs, and the spinal cord so we adopt this image for subsequent steps.

•**Preprocessing.** In this step, image quality is enhanced and initial background marking process is performed. Also, intensity difference between a T1-weighted sagittal slice and a T2-weighted sagittal slice is computed.

– *Image Quality Enhancement.* Image quality is enhanced by median filtering with a window size of 3.

– *Noise attenuation.* Effects of noise are attenuated also by median filtering. Coarse background marking process also reduces substantial amount of noise.

– *Initial background marking.* By forcibly marking pixels on the far left and far right sides, we can decrease the size of foreground regions since the spinal canal is located in the middle of a sagittal image.

– *Computation of intensity difference between a T1-weighted sagittal slice and a T2-weighted sagittal slice.* The difference between the T2-weighted and the corresponding T1-weighted is known to highlight the regions that are high in water content and low in fat content [12]. Thus, we employ this region for subsequent processing. The T1-weighted sagittal slice and the T2-weighted sagittal slice are co-registered in the scanning process by an operator.

•**Reference Generation.** Reference is a left boundary and right boundary of the spinal cord manually marked by a medical expert. To validate the model generated boundary, we need the left boundary and the right boundary of the spinal cord to check if the model-based boundary falls between these two manually-marked boundaries.

•**Validation by the Fréchet Distance.** The Fréchet distance of two curves measures the similarity of the curves. It is frequently used in shape recognition and matching [10], [11].

A *curve* is defined as a continuous mapping $f : [a,b] \to V$, where $a,b \in \mathbb{R}$ and $a \leq b$ and (V,d) is a metric space.

Given two curves $f : [a,b] \to V$ and $g : [x,y] \to V$, their *Fréchet distance* is defined as

$$\delta_F(f,g) = \inf_{\alpha,\beta} \left\{ \max_{t\in[0,1]} d\left(f(\alpha(t)), g(\beta(t))\right) \right\}, \qquad (1)$$

where α and β are arbitrary increasing continuous functions from $[0,1]$ onto $[a,b]$, and $[x,y]$, respectively.

The Fréchet distance between the two arbitrary curves is typically approximated by a polygonal curve. A *polygonal curve* is a curve $P : [0,n] \to V$, where n is a positive integer such that for each $i \in 0,1,\ldots,n-1$, the restriction of P to the interval $[i,i+1]$ is affine.

Let P and Q be polygonal curves and $\sigma(P) = (u_1,\ldots,u_p)$ and $\sigma(Q) = (v_1,\ldots,v_q)$ the corresponding sequences. A *coupling* L between P and Q is a sequence $(u_{a_1},v_{b_1}),\ldots,(u_{a_m},v_{b_m})$ of distinct pairs from $\sigma(P)\times\sigma(Q)$ such that $a_1 = 1, b_1 = 1, a_m = p, b_m = q$, and for all $i = 1,\ldots,q$ we have $a_{i+1} = a_i$ or $a_{i+1} = a_i + 1$, and $b_{i+1} = b_i$ or $b_{i+1} = b_i$. The *length* $\|L\|$ of the coupling L is the length of the longest links in L, i.e., $\|L\| = \max_{i=1,\ldots,m} d(u_{a_i},v_{b_i})$.

Given polygonal curves P and Q, their *discrete Fréchet distance* is defined to be $\delta_{dF}(P,Q) = \{\min \|L\| \mid L$ is a coupling between P and $Q.\}$

B. Dynamic Programming

Dynamic programming is an optimization method based on the principal of optimality [13]. That is, the basic idea behind it is whatever the path to the node A was, there exists an optimal path between node A to the end node.

If a graph has r layers and c nodes, the optimal path to the next level is computed by

$$D\left(x_c^{r+1}\right) = \min_i \left(D\left(x_c^r\right) + f^r(i,c)\right), \tag{2}$$

where $D\left(x_c^{r+1}\right)$ is the updated cost to the node x_c^{r+1} from the first layer and $f^r(i,c)$ is a cost between nodes x_i^r and x_c^{r+1}. For simplicity, we assume that $i \in \{-1,0,1\}$ as in [13]. This computation is continued until one of the end point is reached. Then the optimal path is computed by

$$\min\left(D\left(x^1,\ldots,x^R\right)\right) = \min_{c=1,\ldots,n}\left(D\left(x_c^R\right)\right), \tag{3}$$

where x_c^R are the end nodes, R the number of layers, and $D\left(x^1,\ldots,x^R\right)$ the cost of a path between the first and the last layer. Finally, the optimal path is obtained by back-tracking the node from the last layer to the first layer.

Based on the basic idea, for extraction of the boundary of the spinal canal, we employ two different approaches: one that an initial cost is computed by pixel intensity values and the other based on pixel gradient. The details of each algorithm are as follows.

- **Intensity-based Boundary Extraction.**

STEP 1. Set the initial cost $D(x_j^1)$ for each nodes $j = 1,\ldots,n$ in the first layer by the pixel intensity values and set distance matrix $f^r(j,c)$ to 0 where $r = 1,\ldots,R-1$ and R is the number of layers.

STEP 2. For each $r = 1,\ldots,R-1$, do the following. For each nodes $c = 1,\ldots,n$ in the corresponding layer r compute $D\left(x_c^{r+1}\right) = \min_{i\in\{-1,0,1\}}\left(D\left(x_c^r\right) + f^r(i,c)\right)$.

STEP 3. Find the optimal node x_c^R in the last layer R and find the optimal path from node x_c^R to the node x_j^1 by back-tracking.

- **Gradient-based Boundary Extraction.**

STEP 1. Set the initial cost $D(x_j^1)$ for each nodes $j = 1,\ldots,n$ in the first layer by the gradient by a Sobel edge detector and set distance matrix $f^r(j,c)$ to 0 where $r = 1,\ldots,R-1$ and R is the number of layers.

STEP 2 and STEP 3. The same as the intensity-based boundary extraction algorithm.

III. EXPERIMENT

A. Image Dataset

MRI data from 65 subjects are used in the experiment. Each data contains images in T1-weighted sagittal and T2-weighted sagittal protocol and each slice in different protocols is co-registered. All MR images were taken by a 3-T Philips scanner of 512×512 matrix size. The scanning parameters for all images in T1-weighted protocol are an echo time of 7.2 ms, a repetition time of 530.0 ms, and a slice thickness of 4.5 mm. Similarly, the parameters for all images in T2-weighted protocol are an echo time of 100.0 ms, a repetition time of 2622.4 ms, and a slice thickness of 4.5 mm. The experiments are performed on a machine that has an Intel Core i7 processor with 6GB memory.

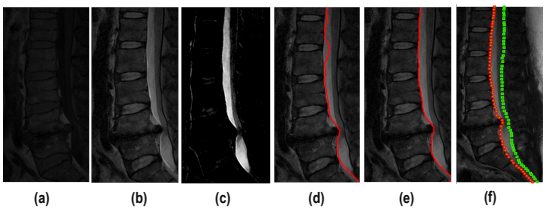

Fig. 2. Whole process. (a) A T1-weighted sagittal image, (b) a T2-weighted sagittal image, (c) difference of intensity between T1- and T2-weighted images, (d) the boundary output generated by the intensity-based method, (e) the boundary output generated by the gradient-based method, and (f) the manually-marked reference boundaries.

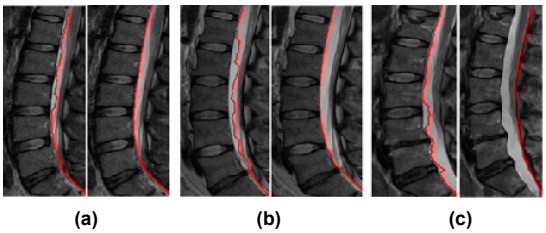

Fig. 3. Several results: (a), (b), and (c). (left) resulting boundaries based on the intensity-based method, and (right) resulting boundaries based on the gradient-based method.

B. Results and Discussion

Fig 2. shows the whole process of the boundary extraction. The Fig. 2(a) and Fig. 2(b) show the T1-weighted and T2-weighted sagittal images. Fig. 2(c) shows the intensity difference between the corresponding slice in each protocol. We can observe that the contrast of the intensity between the spinal canal and the neighboring regions is enhanced. In Fig. 2(d) the boundary is extracted based on the initial intensity value for each pixel while in Fig. 2(e), the boundary is obtained based on the initial edge gradient by a Sobel detector. Fig. 2(f) shows reference boundaries by the medical expert. The initial boundary point is chosen automatically as the one that has the highest intensity value in the first layer or the one having the highest gradient in the first layer. As dynamic programming seeks a minimum cost path, the inverse of intensity difference is fed to a path finding process. Since the center of the spinal cord is usually the brightest (but not always), in most cases the boundary starts within the spinal cord since it has the minimal cost of one row. Fig. 3 shows several results from different patients. Depending on the initial value, both algorithms gives different outputs. In Figs. 3(a)-(c), the outputs from the intensity-based method follow bright regions along the layer, while the outputs from the gradient-based method trace the left or the right boundary of the spinal canal since the gradient values are large along the boundary. The whole path extraction is done automatically. The Table 1 shows that the hit rate computed by the following criterion: Is the boundary by computer

TABLE I

HIT RATE THAT THE BOUNDARY FALLS WITHIN THE SPINAL CANAL

Method type	Intensity-based	Gradient-based
Hit rate	100%	98.5%

TABLE II

MEAN AND STD OF FRÉCHET DISTANCE IN PIXEL FOR EACH METHOD

Intensity-based Method				Gradient-based Method			
Left boundary		Right boundary		Left boundary		Right boundary	
mean	std	mean	std	mean	std	mean	std
13.6	32.2	134.7	33.0	33.6	116.8	134.9	127.9

falls within the left boundary and right boundary of the reference boundaries manually set by a human? The hit rate is defined by the number of boundaries satisfying the above criterion divided by the number of all boundaries in the data set (i.e., 65). As the intensity-initialized method follows the high intensity path from the first row to the last row, it always falls within the spinal canal for all data set. However, the gradient-initialized method moves away from the spinal canal when the gradient between the vertebra and the adjacent regions is large. Also it tends to deviate when the boundary region is blurry and noisy. That is why the intensity-based one works better in terms of the performance metric. This is also confirmed by the mean and standard deviation of Fréchet distance between the computer-generated boundary and the left reference boundary and the right reference for each method in Table 2. Since the gradient-based method tends to generate a boundary close to the left or right boundary of the spinal canal as in Fig. 4, the standard deviation of the Fréchet distance is relatively large (i.e., 32.3 and 33 pixels for the intensity-based method and 116.8 and 127.9 pixels for the gradient-based method). For both methods the extracted boundary tends to close to the left boundary since the brightest pixel in the first row positioned left to the spinal cord and the spinal cord and cauda equina prevent the intensity-based path from moving toward the right boundary. This is confirmed by the mean distance that is small for both cases (i.e., 13. 6 pixels $<$ 134.7 pixels and 33.6 pixels $<$ 134.9 pixels). The distance of 13.6 pixels indicates two curves match almost perfectly. The elapsed time for generating the left reference boundary and the right boundary is 48.6 ± 2.4 secs and 46.4 ± 4.1 secs, respectively. The elapsed time for the intensity-based method is 0.8 ± 0.2 secs and the time for the gradient-based method method is 0.9 ± 0.4 secs. Due to the computation of gradient requires extra time, the gradient-based method takes more time than the intensity-based one. Different than our previous results for the spinal canal segmentation [15], [16], the extracted boundary reaches the bottom of the image whereas the previous ones extract the spinal cord only when the distinction of the intensity of gradients are obvious in the border. The extracted boundary that falls within the spinal canal is used as a landmark to mark background areas, to localize neighboring vertebrae and intervertebral discs, and to diagnose spondylolisthesis. Since the detected boundary is sometimes odd and somewhere between the left and right spinal canal boundaries, a more sophisticated boundary detection algorithm needs to be applied to extract an exact boundary of the spinal canal.

IV. CONCLUSIONS

To meet the need for computer-aided diagnosis and characterization, we have developed a computer-aided diagnosis and characterization framework in the lumbar spine MRI that includes the spinal cord, vertebrae, and intervertebral discs. In this paper, we propose two spinal cord boundary tracing methods based on dynamic programming in lumbar spine MRI to be fit into our CAD framework. Our method fuses the intensity of the image and the gradient of the image into a dynamic programming scheme and works in a fully-automatic fashion. The boundaries generated by our method is compared against reference boundaries in terms of Fréchet distance which is known to be a metric for shape analysis. The experimental results from 65 clinical data show that our methods find the boundary with a hit rate of 99%.

REFERENCES

[1] M. Bhargavan, J. H. Sunshine, and B. Schepps, "Too few radiologists?," Am. J. Roentgenol. , vol. 178, no. 5, pp. 1075-1082, 2002.

[2] K. Doi and H. K. Huang, "Computer-aided diagnosis (CAD) and image-guided decision support," Computerized Medical Imaging and Graphics, vol. 31, pp. 195-197, 2007.

[3] D. Geiger, A. Gupta, L. A. Costa, and J. Vlontzos, "Dynamic Programming for Detecting, Tracking, and Matching Deformable Contours," IEEE Trans. PAMI, vol. 17, no. 3, pp. 294-302, 1995.

[4] Q. Liang, I. Wendelhag, J. Wikstand, and T. Gustavsson, "A Multiscale Dynamic Programming Procedure for Boundary Detection in Ultrasonic Artery Image," IEEE Trans. on Medical Imaging, vol. 19, no. 2, pp. 127-141, 2000.

[5] C. Kirbas, and F. Quek, "A Review of Vessel Extraction Techniques and Algorithms," ACM Comput. Surv., vol. 36, pp. 81-121, 2004.

[6] B.D. Schmit and M.K. Cole, "Quantification of Morphological Changes in the Spinal Cord in Chronic Human Spinal Cord Injury using Magnetic Resonance Imaging", EMBS, pp. 4425-4428, 2004.

[7] R.V. Uitert, I. Bitter, and J.A. Butman, "Semi-Automatic Spinal Cord Segmentation and Quantification", CARS, pp. 224-229, 2005.

[8] C. McIntosh and G. Hamarneh, "Spinal Crawlers: Deformable Organisms for Spinal Cord Segmentation and Analysis", MICCAI 2006, vol. 4190, pp. 808-815, 2006.

[9] M.A. Horsfield, S. Sala, M. Neema, M. Absinta, A. Bakshi, M.P. Sormani, M.A. Rocca, R. Bakshi, and M. Filippi, "Rapid Semi-Automatic Segmentation of the Spinal Cord from Magnetic Resonance Images: Application in Multiple Sclerosis", NeuroImage, vol. 50, pp. 446-455, 2010.

[10] H. Alt and M. Godau, "Computing the Fréchet distance between two polygonal curves," International Journal of Computational Geometry and Applications, vol. 5, pp. 75-91, January 1995.

[11] B. Aronov, S. Har-Peled, C. Knauer, Y. Wang, and C. Wenk, "Fréchet distance for curves, revisited," Proceedings of the 14th Annual European Symposium on Algorithms, vol. 14, pp. 52-63 , 2006.

[12] C. Bhole, S. Kompalli, and V. Chaudhary, "Context-sensitive labeling of spinal structures in MRI images," Proc. SPIE, pp. 72603P, 2009.

[13] M. Sonka, M. Hlavac, and R. Boyle, Image Processing, Analysis, and Machine Vision, Thompson Learning, 2008.

[14] H. Gray, Anatomy of the Human Body , Bartley, 2000, available at `http://www.bartleby.com/107/illus661.html`.

[15] J. Koh, T. Kim, V. Chaudhary, G. and Dhillon, "Automatic Segmentation of the Spinal Cord and the Dural Sac in Lumbar MR Images Using Gradient Vector Flow Field," EMBC'10, pp. 2117-2120, 2010.

[16] J. Koh, P. D.Scott, V. Chaudhary, and G. Dhillon, "An Automated Segmentation Method of the Spinal Canal From Clinical MR Images Based on an Attention Model and an Active Contour Model," ISBI'11, pp. 1467-1471, 2011.